Advanced Compact MOSFET Model HiSIM2 Based on Surface Potentials with a Minimum Number of Approximation

M. Miura-Mattausch, D. Navarro, N. Sadachika, G. Suzuki, Y. Takeda, M. Miyake,
T. Warabino, K. Machida, T. Ezaki, H. J. Mattausch
*T. Ohguro, *T. Iizuka, *M. Taguchi, *S. Kumashiro, *R. Inagaki, and *S. Miyamoto
Grad. School of Adv. Sc. of Matter, Hiroshima Univ.,739–8530, Japan, mmm@hiroshima-u.ac.jp
* Semiconductor Technology Academic Research Center 3-17-2 Shin-Yokohama, Kanagawa, 222-0033, Japan

Abstract

The compact MOSFET-model development trend leads to models based on the channel surface potential, allowing higher accuracy and a reduced number of model parameters. Among these only HiSIM solves the surface potentials with an efficient, physically correct iteration procedure, avoiding additional approximations without any computer run-time penalty. It is further demonstrated that excellent model accuracy for higher-order phenomena, which is a prerequisite for accurate RF circuit simulation, is achieved by HiSIM without any new model parameters in addition to those for describing the I-V characteristics.

Keywords: MOSFET Model, Surface Potential, Analog & RF Application

1 Introduction

MOSFET technology is leading semiconductor industries through aggressive size reduction on a short time scale. To achieve further scaling down, also improvement of the device structure has been undertaken such as in multi-gate MOSFETs [1], [2]. Application of advanced MOSFETs to circuits is an additional urgent task to meet required high circuit performances. For this purpose compact models of the MOSFET devices are indispensable.

As microscopic device phenomena are becoming dominant for device features [3], compact models cannot ignore the physics behind the phenomena any more. Otherwise the model cannot predict device features accurately and also the enormous increase of the number of model parameters cannot be stopped. It is shown that surface-potential-based modeling is the first step to get a breakthrough toward an improved situation [4]. HiSIM (Hiroshima-university STARC IGFET Model) is the first complete MOSFET model for advanced technologies developed based on the concept [5]–[7]. Measurements of higher-order device features, important for analog as well as RF circuits, are shown to provide insight of microscopic carrier dynamics, which is very useful for developing accurate models [8].

2 Surface-Potential Calculation

All device featuers are determined by the surface-potential distribution along the channel $\phi_{\rm s}(y)$, which is calculated by solving the Poisson equation with the Gauss law [9]

$$C_{\rm ox}\big(V'_{\rm G}-\phi_{\rm S}(y)\big)=\sqrt{\frac{2\epsilon_{\rm Si}qN_{\rm sub}}{\beta}} \Bigg[\exp\big\{-\beta(\phi_{\rm S}(y)-V_{\rm bs})\big\}+\beta(\phi_{\rm S}(y)-V_{\rm bs})-1 +\frac{n_{\rm p0}}{p_{\rm p0}}\Big\{\exp\big(\beta(\phi_{\rm S}(y)-\phi_{\rm f}(y))\big)-\exp\big(\beta(V_{\rm bs}-\phi_{\rm f}(y))\big)\Big\}\Bigg]^{\frac{1}{2}} \tag{1}$$

$$C_{\rm ox}=\frac{\epsilon_{\rm ox}}{T_{\rm ox}} \tag{2}$$

$$V'_{\rm G}=V_{\rm gs}-V_{\rm fb} \tag{3}$$

$$\beta=\frac{q}{kT} \tag{4}$$

$$\phi_{\rm f}(L_{\rm eff})-\phi_{\rm f}(0)=V_{\rm ds} \tag{5}$$

$$n_{\rm p0}=\frac{n_{\rm i}^2}{p_{\rm p0}} \tag{6}$$

where $V_{\rm fb}$ is the flat-band voltage, and $T_{\rm ox}$ is the physical gate-oxide thickness. The hole concentration at equilibrium condition $p_{\rm p0}$ is approximated to be the substrate impurity concentration $N_{\rm sub}$. The quasi-Fermi potential $\phi_{\rm f}(y)$ together with $V'_{\rm G}$ determines the carrier concentration in the channel. The intrinsic carrier concentration $n_{\rm i}$ is

$$n_{\rm i}=n_{\rm i0}T^{\frac{3}{2}}\exp\left(-\frac{E_{\rm g}}{2q}\beta\right)\ , \tag{7}$$

where $E_{\rm g}$ describes the temperature dependent bandgap. Two approximations allow to derive an analytical formulation for all device performances as a function of surface potentials at the source side $\phi_{\rm S0}$ and the drain side $\phi_{\rm SL}$, where $\phi_{\rm SL}$ gives the value at the end of the gradual-channel approximation. The remaining potential increase of $V_{\rm ds}-\phi_{\rm SL}$ in amount occurs both in the pinch-off region and the overlap region as indicated in Fig. 1 [10].

HiSIM solves the Poisson equation iteratively in the same way as numerical device simulators [11]. Other ad-

vanced surface-potential models such as PSP (by Pennsylvania State University and Phillips) approximates the surface potential by explicit mathematical functions with applied voltages as variables [12]. The reason for approximating with closed form equations is to reduce simulation time by eliminating otherwise unavoidable iterations. However, in practical application, the simulation time of the iterative HiSIM approach turns out to be shorte and more accurate than for an analytical approach [4], [13].

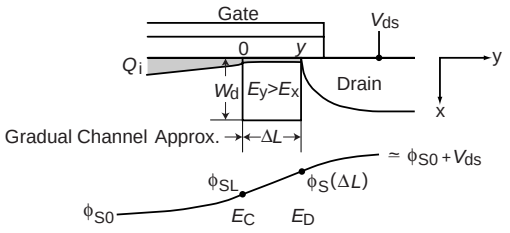

Fig. 1: Schematic showing the correlation among physical quantites in the pinch-off region.

Derivatives of all device characteristics influence strongly analog as well as RF-circuit performances. The features of those derivatives are mainly determined by the surface-potential derivatives with respect to all possible applied voltages. Surface-potential values of HiSIM are compared with 2D-device simulation results in Fig. 2. The slight quantitative differences are explained by the fact, that the impurity profile, used for 2D-device simulations, is not calibrated to the studied devices. Calculated surface-potential derivatives from HiSIM are compared with 2D numerical device simulation results in Fig. 3.

3 Modeled Phenomena

Table 1 summarizes all phenomena modeled in HiSIM2. Most of the phenomena are observed in any type of device geometries for advanced technologies.

3.1 Short-Channel Effects

Different from the drift approximation, the drift-diffusion approximation does not require the threshold voltage $V_{\rm th}$ as a model parameter for describing device characteristics. The MOSFET device parameters such as $T_{\rm ox}$ and $N_{\rm sub}$ determine the complete MOSFET behavior including the subthreshold characteristics automatically and consistently. However, $V_{\rm th}$ provides a good measure for characterizing MOSFET features by shift $\Delta V_{\rm th}$ of $V_{\rm th}$ for short-channel transistors in comparison to the threshold voltage of a long-channel transistor. For example, the pocket-implant technology causes an inhomogeneity of the impurity concentration along the channel. Two model parameters (LP: length of the

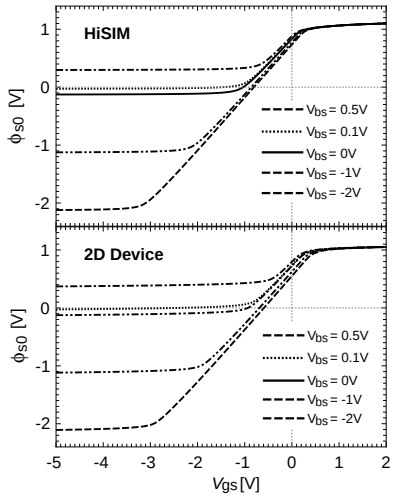

Fig. 2: Comparison of calculated surface potentials at source side $\phi_{\rm S0}$ by HiSIM and a 2D-device simulator for various substrate voltages $V_{\rm bs}$ at a drain voltage of $V_{\rm ds}$=0.1V. Gate length is fixed to 2μm.

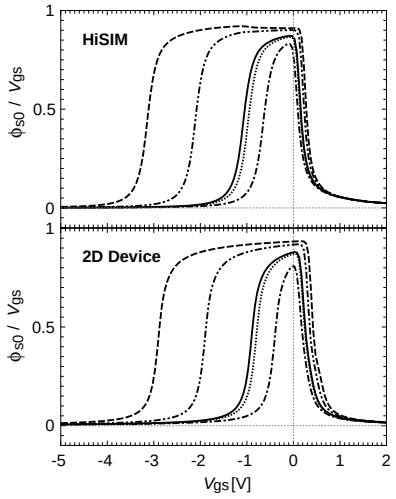

Fig. 3: Comparison of calculated derivatives of the surface potential at source side $\phi_{\rm s0}$ by HiSIM and a 2D-device simulator. Bias conditions are the same as those given in Fig. 2.

pocket extension into the channel; $N_{\rm SUBP}$: peak of the pocket impurity concentration) are introduced as shown in Fig. 4 [14]. Fig. 5 compares the $V_{\rm th}$-$L_{\rm gate}$ characteristics of the developed pocket-implant model with and without inclusion of the short-channel effects (SCE). The steep increase at $L_{\rm gate}$=0.1μm in Fig. 5a means the starting of the pocket overlap, where LP=0.05μm. The short-channel and reverse-short-channel effects are incorporated as the threshold voltage shift together with poly-depletion and narrow width effects, and the poisson equation is solved by including this shift.

Table 1: Modeled phenomena in HiSIM.

Phenomena	Subjects
Short Channel Reverse-Short Channel	 impurity pile-up pocket implant
Poly-Depletion Quantum-Mechanical Channel-Length Modulation Narrow-Channel	
Non-Quasi-Static	Transient Time-Domain AC Frequency-Domain
Temperature Dependency	Thermal Voltage Bandgap Intrinsic-Carrier Concentration Phonon Scattering Maximum Velocity
Mobility Models	Universal Mobility High-Field Mobility
Shallow-Trench Isolation	Threshold Voltage Mobility Leakage Current
Capacitacnes	Intrinsic Overlap Lateral-Field Induced Fringing
Noise	1/f Noise Thermal Noise Induced Gate Noise Cross-Correlation Noise
Leakage Currents	Substrate Current Gate Current GIDL Current
Source/Drain Resistances Junction Diode	 Currents Capacitances

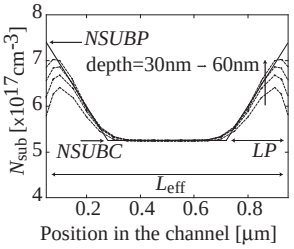

Fig. 4: The dashed curves are simulated impurity profiles by the 2D-process simulator at various depths. The extracted pocket profile with the HiSIM model is depicted by a solid line.

3.2 Mobility Model

The low-field mobility is described with the three independent mechanisms of Coulomb, phonon and surface-roughness scattering, which have been proved to preserve the universality [15]. To preserve the universality in a compact model is a proof for the consistency of the model description (see Fig 6). This is also important for reliable parameter extraction.

3.3 Symmetry Aspects and Scalability

The $V_{\rm ds}$ sweep from positive to negative values changes the direction of the drain current flow. However, the derivatives must be the same, namely symmetry across $V_{\rm ds}$=0 has to be preserved without discontinuity. The surface-potential-based modeling, which includes both

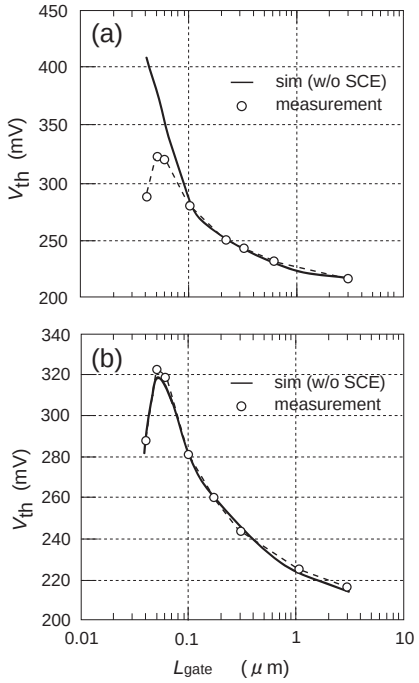

Fig. 5: Comparison of measurements and HiSIM's pocket-implant model for $V_{\rm th}$ as a function of $L_{\rm gate}$. Results (a) with and (b) without short-channel effects (SCE) are shown.

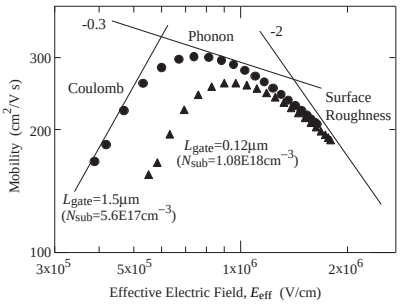

Fig. 6: Calculated mobility as a function of the effective field for different MOSFET devices.

the drift and diffusion contributions, in principle preserves the symmtery automatically. However, the fundamental nature of the symmetry is distroyed by artifacts introduced in modeling phenomena observed in advanced MOSFETs technologies such as short-channel effects. Instead of modeling a diminishing magnitude of the short-channel effect as $V_{\rm ds}$ approaches zero, efficient numerical smoothing is done to improve such unavoidable disturbances [11].

Simulation-time efficient HiSIM, proved to provide stable circuit simulations for large-scale circuits with 1 million devices, makes it possible to extend the SPICE simulation even to very large circuits. Advantage of the evolutional modeling approach based on the surface-potential description over the conventional $V_{\rm th}$-based de-

scription is that the concept is extendable to any advanced MOSFET technology. HiSIM-SOI has been successfully developed based on the same concept but solving three surfaces simultaneously. Calculating the three surface potentials requires only about 2 times more simulation time than for he bulk case in the present development stage [16].

4 Features Supporting RF Applications

Typical phenomena include harmonic distortion, noise, and carrier response delay, which are overviewed here.

4.1 Harmonic Distortion

The harmonic distortion is originated by non-linearity of the device response to applied voltages, which induces additional outputs. If the model is consistent and all model parameters are accurately extracted from measurements, harmonic distortion should be reproduced without any additional model parameters. It has been verified that the low frequency harmonic distortions is indeed correctly reproduced without additional parameters or adjustments. Singularities observed in the harmonic distortions can be attributed to those of the mobility for low $V_{\rm ds}$ values. At high frequencies the harmonic distortion characteristics are governed by carrier dynamics rather than by the mobility alone [17]. Fig. 7 shows calculated IP3 in comparison with measurements.

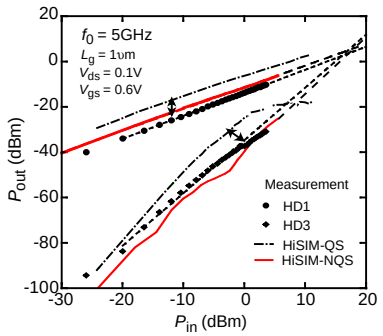

Fig. 7: Harmonic distortion characteristics at 5GHz. HiSIM-NQS predicts the same characteristics as measurements.

4.2 Noise

Advanced MOSFETs are suffering from two dominating noise contributions: the $1/f$ noise and the thermal noise. Additionally frequency dependent induced gate noise and the cross-correlated noise are observed in high-frequency operation [18]. The $1/f$ noise is caused by the carrier fluctuation resulting from trap/detrap processes at the oxide/substrate interface as well as the mobility fluctuation due to the traps. Thus modeling of the noise requires to integrate the carrier distribution along the channel and leads to a formula which depends on carrier concentration at source and drain [19]. Simulation results are compared with measurements in Fig. 8. One model parameter, the trap density, is fitted to the measurements. Modeling of the thermal noise is based

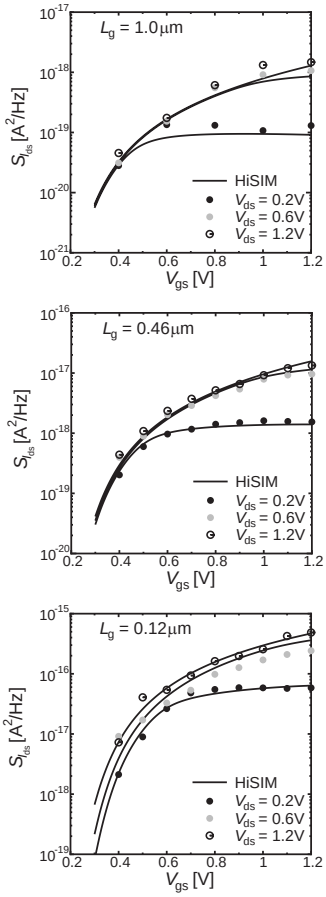

Fig. 8: Comparison of the bias dependence of measured and simulated drain current noise by HiSIM at a frequency of 100Hz.

on the Nyquist theorem considering the noise source as a resistance. This theory is extended to the transistor by van der Ziel, where the thermal noise is the integration of the channel conductance along the channel [18]. In HiSIM the integration is performed with the surface potential $\phi_{\rm s}$ instead of the channel position [20].

The thermal noise is verified with the noise coefficient γ, which is defined as the noise value normalized with the channel conductance at V_{ds}=0. Theoretically it is predicted for long-channel transistors that γ reduces from 1 to 2/3 under the saturation condition. Fig. 9 shows predicted thermal noise coefficients with HiSIM in comparison to measurements [20] for two different technologies.

The increase of the noise coefficient under the saturation condition with reducing the gate length is attributed to the potential gradient increase along the channel.
In addition to the two major noise contributions, induced gate noise and noise cross-correlation are becoming important when operating MOSFETs in higher frequency regimes. This is also modeled in the same way as the other noises, namely by integrating gate conductance along the channel induced by capacitive coupling with the channel conductance [21].
Here it is worthwhile to notice that model parameters are required only for the $1/f$ noise to describe the trap density and the mobility fluctuation due to the traps. These parameters are nearly universal, if the technology is mature [19]. Thus most of the higher-order phenomena can be predicted by the commonly measured I-V characteristics. This fact concludes that the majority of the carrier dynamics even in a microscopic aspect is still governed by electrostatic effects, which are determined by the Poisson equation [8].

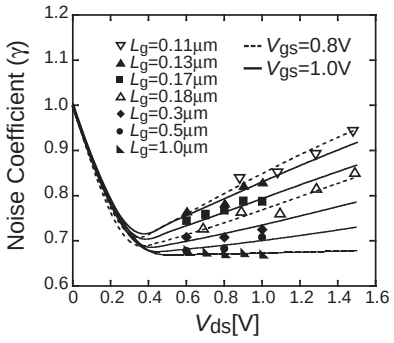

Fig. 9: Calculated noise coefficient γ with HiSIM as a function of drain voltage V_{ds} compared with measurements. Two different technologies are compared. For one technology measurements are represented by solid symbols and corresponding HiSIM results by solid lines, and for the other technology by open symbols and dashed lines.

4.3 Non-Quasi-Static Effects

The modeling including the non-quasi-static (NQS) effect is done in HiSIM by considering the carrier transit delay [22]. Simulation time increase of only about 3% in comparison with the QS approximation is achieved without sacrificing accuracy of the simulation result. For circuits, where the NQS effect is obvious, even simulation time reduction has been observed [23]. Advantage of HiSIM is an easy to perform NQS simulation, just by selecting the model flag provided in HiSIM. To derive a closed form equation based on the origin of the high frequency response instead of using a substrate network, the continuity equation is solved together with the current density equation in an analytical way. The final description reduces to an expression of the Bessel functions [24], which can be extended to the surface-potential description including the drift and diffusion contributions [25], called HiSIM-SSA. Comparisons of model calculation results and measurements are shown in Fig. 10 without the gate resistance contribution. The NQS effect becomes obvious at frequencies beyond 1/3 of the cut-off frequency. A unified NQS

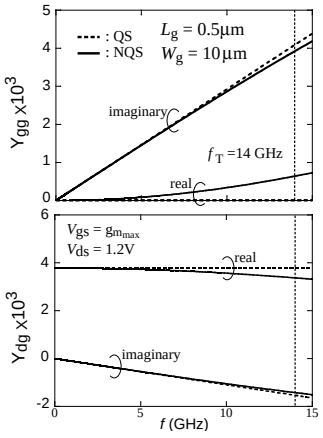

Fig. 10: Measured (open symbols) and calculated Y-parameters with the NQS model (solid lines) and the QS model (dashed lines) without the gate-resistance contribution.

model both for transient analysis and AC analysis is desired to extend the simulation capability. This enables high-frequency verification done for both the time-domain and the frequency-domain aspects at the same time without additional effort. For this purpose the Fourier transformation of the transient NQS model is the most straightforward approach. Therefore, we derived an analytical formulation for the frequency domain analysis based on the Fourier transformation. The result is shown in Fig. 11 in comparison with the numerical Fourier transformation of the time-domain result. Good agreement of the two methods up to the frequencies of 2 times the cut-off frequency proves validity of the method for real applications [26]. Thus HiSIM includes the following options. One is to select the QS or NQS model, and the other is to select the time-domain or frequency-domain analysis. Here it is emphasized again that a parameter extraction with only the I-V characteristics is sufficient even for the NQS simulation. It has to be noticed that HiSIM's NQS model allows to describe all MOSFET related RF effects without any additional parameters, whereas this was previously only possible by extracting the elements of a substrate-resistance network from Y-parameter measurements.

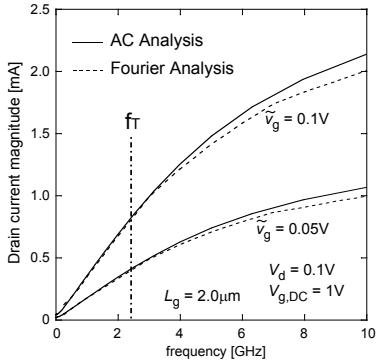

Fig. 11: Comparison of drain current magnitude calculated with frequency-domain model and time-domain model.

5 CONCLUSION

The development trend in compact modeling goes towards surface-potential based approaches and leads to models with high accuracy and less model parameters. The main motivation for this trend is to realize RF circuits with MOSFETs, where many higher-order phenomena affect the circuit performance. The surface-potential-based description brings compact modeling much closer to reality. This is because the surface potentials, solutions of the Poisson equation, provide the device-physical basis for deriving all possible MOSFET features. HiSIM is an advanced MOSFET model, which turns these principles into practical reality.

REFERENCES

[1] K. Ishii, Y. Hayashi and T. Sekigawa, *Jpn. J. Appl. Phys.*, vol. 29, pp. 521, 1990.

[2] K. K. Hung, P. K. Ko, C. Hu, and Y. C. Cheng, *IEEE Trans. Electron Devices*, vol. 37, No. 5, pp. 1323, 1990.

[3] S. E. Laux, *Tech. Digest IEDM*, pp. 135, 2004.

[4] M. Miura-Mattausch, U. Feldmann, A. Rahm, M. Bollu, and D. Savignac, *IEEE Trans. CAD/ICAS*, vol. 15, No. 1 pp. 1, Jan. 1996.

[5] M. Miura-Mattausch, H. J. Mattausch, N. D. Arora, and C. Y. Yang, *IEEE Circuits and Devices*, vol. 17, No. 6, pp. 29, 2001.

[6] M. Miura-Mattausch, H. Ueno, M. Tanaka, H. J. Mattausch, S. Kumashiro, T. Yamaguchi, K. Yamashita, and N. Nakayama, *Tech. Dig. IEDM*, pp. 109, 2002.

[7] M. Miura-Mattasuch, H. Ueno, H. J. Mattausch, K. Morikawa, S. Itoh, A. Kobayashi, and H. Masuda, *IEICE Trans. Electron.*, vol. E86-C, No. 6, pp. 1009, 2003.

[8] M. Miura-Mattausch, *Proc. SISPAD*, pp. 1, 2005.

[9] H. C. Pao and C. T. Sah, *Solid-State Electron.*, vol. 9, pp. 927, Oct. 1966.

[10] D. Navarro, T. Mizoguchi, M. Suetake, K. Hisamitsu, H. Ueno, M. Miura-Mattausch, H. J. Mattausch, S. Kumashiro, T. Yamaguchi, K. Yamashita, and N. Nakayama, *IEICE Trans. Electron.*, vol. E88-C, No. 5, pp. 1079, 2005.

[11] HiSIM1 Users Manual, Hiroshima University and STARC, 2002.

[12] G. Gildenblat, X. Li, H. Wang, W. Wu, R. van Langevelde, A. J. Scholten, G. D. J. Smit and D. B. M. Klaassen, *Tech. Proc. WCM*, pp. 19, 2005.

[13] R. Rios, S. Mudanai, W. -K. Shih and P. Packan, *Tech. Digest IEDM*, pp. 755, 2004.

[14] H. Ueno, D. Kitamaru, K. Morikawa, M. Tanaka, M. Miura-Mattausch, H. J. Mattausch, S. Kumashiro, T. Yamaguchi, K. Yamashita, and N. Nakayama, *IEEE Trans. Electron Devices*, vol. 49, pp. 1783, 2002.

[15] A. G. Savinis and J. T. Clemens, *Tech. Digest IEDM*, pp. 18, 1979.

[16] N. Sadatika, Y. Uetsuji, D. Kitamaru, H.J. Mattausch, M. Miura-Mattausch, L. Weiss, U. Feldmann, and S. Baba, *Proc. SISPAD*, pp. 251, 2004.

[17] Y. Takeda, D. Navarro, S. Chiba, M. Miura-Mattausch, H. J. Mattausch, T. Ohguro, T. Iizuka, M. Taguchi, S. Kumashiro, and S. Miyamoto, *Proc. CICC*, pp. 827, 2005.

[18] A. van der Ziel, "Noise in Solid Sate Devices and Circuit," New York, John Wiley & Sons, Inc., 1986.

[19] S. Matsumoto, H. Ueno, S. Hosokawa, T. Kitamura, M. Miura-Mattausch, H. J. Mattausch, T. Ohguro, S. Kumashiro, T. Yamaguchi, K. Yamashita and N. Nakayama, *IEICE Trans. Electron.*, vol. E88-C, No. 2, pp. 247, 2005.

[20] S. Hosokawa, D. Navarro, M. Miura-Mattausch, H. J. Mattausch, T. Ohguro, T. Iizuka, M. Taguchi, S. Kumashiro, and S. Miyamoto, *Appl. Phys. Lett.*, vol. 87, article 092104, 2005.

[21] T. Warabino et al., submitted for publication.

[22] N. Nakayama, D. Navarro, M. Tanaka, H. Ueno, M. Miura-Mattausch, H. J. Mattausch, T. Ohguro, S. Kumashiro, M. Taguchi, T. Kage, and S. Miyamoto, *Electronics Letters*, vol. 40, pp. 276, 2004.

[23] D. Navarro et al., submitted for publication.

[24] J. J. Paulos and D. A. Antoniadis, *IEEE Electron Device Lett.*, vol. EDL-4, pp. 221, 1983.

[25] S. Jinbou, H. Ueno, H. Kawano, K. Morikawa, N. Nakayama, M. Miura-Mattausch, and H. J. Mattausch, *Ext. Abs. SSDM*, pp. 26, 2002.

[26] K. Machida, D. Navarro, M. Miyake, R. Inagaki, N. Sadachika, T. Ezaki, H. J. Mattausch, M. Miura-Mattausch, *Proc. Silicon Monolithic Integrated Circuits in RF Systems*, pp. 73, Jan. 2006.